13962

OPSEC REVIEW CERTIFICATION

(AR 530-1, Operations Security)

I am aware that there is foreign intelligence interest in open source publications. I have sufficient technical expertise in the subject matter of this paper to make a determination that the net benefit of this public release outweighs any potential damage.

Reviewer: _Ernest R. Schwarz_ _GS-15_ _TL_ _Prop. Rsch_
     Name   Grade Title _TARDEC_

Ernest C. Schwarz   _12/9/03_
  Signature   Date

Description of Information Reviewed:

Title: _A Methodology for Indirect Determination of Diesel Fuel Laminar Flame Speed_

Author/Originator(s): _Peter Schihl, John Tasdemir_

Publication/Presentation/Release Date: _March, 2004_

Purpose of Release: _SAE International Congress_

An abstract, summary, or copy of the information reviewed is available for review.

Reviewer's Determination (circle one):

 (1.) Unclassified Unlimited.

 2. Unclassified Limited, Dissemination Restrictions IAW _____.

 3. Classified. Cannot be released, and requires classification and control at the level of _____.

Security Office (AMSTA-CS-S):

(Concur)/Nonconcur _____   _19 DEC 2003_
     Signature   Date

Public Affairs Office (AMSTA-CS-Cf):

(Concur/Nonconcur _____   _22 Dec 03_
    Signature   Date

2004-01-0930

A Methodology for Indirect Determination of Diesel Fuel Laminar Flame Speed

Peter Schihl and John Tasdemir
U.S. Army TARDEC Propulsion Laboratory

ABSTRACT

A method for indirectly determining the laminar flame speed for diesel fuel was formulated and benchmarked against cylinder pressure data acquired for two direct-injection diesel engines. The approach was focused on fitting a series of experimentally generated heat release and mean cylinder pressure profiles with a zero-dimensional, physics-based combustion model. A correlation for laminar flame speed was generated based on the optimal fit of flame speed to this series of heat release profiles. This technique resulted in a correlation that had a reasonable RMS error and exhibited trends that have been observed with lighter hydrocarbon fuels such as gasoline including pressure and air fuel ratio behavior.

INTRODUCTION

Laminar flame speed is an important diesel combustion parameter given the nature of the initial energy release rise of the heat release event – the premixed phase. Small scale turbulence generated by the spray is controlled by the injection rate and nozzle geometry that in turn impacts the overall turbulent energy spectrum and thus the Taylor or dissipation scale. In this study, peak injection pressures were fairly high (900 – 1200 bar), thus leading to fine small scale turbulence that allows for use of the flamelet assumption [1] during the initial stage of energy release. In this sense, if the reaction time across the dissipation scale eddies is known then determination of the average burn rate becomes a function of flame front entrainment rate. For a real world diesel spray scenario, the dissipation scale is a function of position and time thus leading toward a full three-dimensional flow field solution that is highly dependent on the type of turbulence closure approach.

In order to maintain a zero-dimensional philosophy for determining the average premixed phase burning rate, turbulence must be isotropic and thus a priori knowledge of the turbulent large scale or bulk mixing length will dictate the dissipation scale. Furthermore, this large scale must be determined based on combustion system design in order to fulfill the isotropy assumption. In this paper, the large scale is assumed to vary with specific geometric dimensions that dictate the large scale mixing rate. *Thus it is possible to predict the burning rate profile with a priori knowledge of the laminar flame speed for DF-2 over both relevant combustion chamber temperature and pressure ranges through utilization of the flamelet assumption.*

Much effort has been spent in the past measuring laminar flame speed for lighter hydrocarbon fuels. Such efforts typically have included methane, ethylene, ethane, di-methyl ether and propane [2-8] over a range of equivalence ratios, but typically at near atmospheric pressure and lower temperatures in comparison to a diesel-like environment. Correlations for laminar flame speed do exist for gasoline surrogates [9] and are limited to C_8 representation. A recent effort to measure this key parameter for DF-2 was unsuccessful at the boiling point (one atmosphere) due to pre-ignition of the charge [10]. The main issue with this particular measurement from a macroscopic viewpoint is the high cetane number in comparison to more volatile fuels such as gasoline, i.e. reduction in ignition delay. Preparation of a homogeneous charge involves some type of mixing process that inherently results in pre-ignition even at temperatures and pressure much less than typical light-load diesel conditions.

One possible solution is to extrapolate a correlation developed for lighter hydrocarbon fuels such as iso-octane [11]. Such an approach is limited by both an equivalence ratio of one and a half [9], since predicted laminar flame speeds become negative under richer conditions, and also failure to account for the higher molecular weight (diffusivity) of a typical DF-2 (~210 g/gmole versus 116 g/gmole for iso-octane) which tends to attenuate laminar flame speed [9]. Past optical engine experiments have shown that the premixed phase mixing layer has an average equivalence ratio greater than one and a half under various operating conditions [12-14] and thus extrapolation of iso-octane laminar flame correlations is not feasible without major modification to the pressure and/or equivalence ratio exponent [11].

Another solution is to calibrate a combustion model over a large sample of experimentally determined heat

Report Documentation Page

1. REPORT DATE **12 DEC 2003**	2. REPORT TYPE **N/A**	3. DATES COVERED **-**	
4. TITLE AND SUBTITLE **A Methodology for Indirect Determination of Diesel Fuel Laminar Flame Speed**		5a. CONTRACT NUMBER	
		5b. GRANT NUMBER	
		5c. PROGRAM ELEMENT NUMBER	
6. AUTHOR(S) **Schihl, Peter; Tasdemir, John**		5d. PROJECT NUMBER	
		5e. TASK NUMBER	
		5f. WORK UNIT NUMBER	
7. PERFORMING ORGANIZATION NAME(S) AND ADDRESS(ES) **USA TACOM 6501 E. 11 Mile Road Warren, MI 48397-5000**		8. PERFORMING ORGANIZATION REPORT NUMBER **13962**	
9. SPONSORING/MONITORING AGENCY NAME(S) AND ADDRESS(ES)		10. SPONSOR/MONITOR'S ACRONYM(S) **TACOM TARDEC**	
		11. SPONSOR/MONITOR'S REPORT NUMBER(S)	
12. DISTRIBUTION/AVAILABILITY STATEMENT **Approved for public release, distribution unlimited**			
13. SUPPLEMENTARY NOTES **U.S. government Work; not copyrighted in the U.S. Presented at SAE World Congress 2004**			
14. ABSTRACT			
15. SUBJECT TERMS			

16. SECURITY CLASSIFICATION OF:			17. LIMITATION OF ABSTRACT **SAR**	18. NUMBER OF PAGES **8**	19a. NAME OF RESPONSIBLE PERSON
a. REPORT **unclassified**	b. ABSTRACT **unclassified**	c. THIS PAGE **unclassified**			

release rate profiles through modulation of the laminar flame speed. In this sense the model could be fit to the premixed phase under the assumption that the mixing layer fuel consumption rate is predominately dictated by laminar flame speed if TURBULENCE INTENSITY is known or predictable in semi-accurate fashion. This latter condition is met if the model also accurately predicts the mixing-controlled phase since this event is primarily a function of the turbulence intensity. Such an effort requires judicious selection of other possible spray parameters (spray angle, nozzle discharge coefficient, and the turbulent dissipation constant) that may affect the premixed burn phase profile, but utilization of a large experimental heat release database should minimize this effect.

EXPERIMENTAL SETUP

Two direct injection diesel engines were employed for this study as shown in table 1. The smaller bore engine was a single cylinder automotive-type [15] while the larger bore engine was a two cylinder engine whose eight cylinder predecessor is employed in a combat vehicle application [16]. Each engine was operated over a variety of speed and load conditions, and included necessary instrumentation to obtain in-cylinder pressure for heat release analysis. Additionally, the smaller bore engine was also operated at various exhaust recirculation (EGR) levels, fuel injection pressures, and injection timing schedules.

Table 1: Engine Specifications

Engine Parameter	Description	
	Cummins V903	Ford DIATA
Model Type	Cummins V903	Ford DIATA
Number of Cylinders	2	1
Injection system	PT	FEV CORA II
Injection pressure[1] (bar)	600 – 1300	500 –1200
Nozzle geometry (mm)	7 x 190	6 x 0.124
Bore x stroke (mm)	140 x 125	70 x 78
Compression ratio	12.5	19.5
Swirl number	0.8	2.4[3]
Displacement[4] (cc)	1850	300
Operating speeds (rpm)	1600 - 2600	1500 – 3000
IMEP range (bar)	5 – 14	3 – 18
Boost system	Shop air	

[1] Peak value.
[2] Flow bench demonstration at maximum valve lift.
[3] Per cylinder.

Heat release analysis was performed using standard thermodynamic first law analysis and the ideal gas law. The specific heat ratio was calculated based on an ideal gas mixture of CO_2, H_2O, N_2, O_2 and gaseous diesel fuel when appropriate, i.e. after start of injection, and the bulk cylinder temperature was determined based on corrected real gas behavior [17] and estimated in-cylinder charge mass – the corresponding equation of state is given by:

$$v = \frac{RT}{P} + 1.09059\, x10^{-3} - \frac{8.50053x10^{-3}}{(T/100)^{1.64}} + \frac{4.34248x10^{-10}}{(T/100)^{2.49}}P - \frac{6.52579x10^{-18}}{(T/100)^{2.92}}P^2 + \frac{2.95689x10^{-26}}{(T/100)^{3.17}}P^3 \quad (1)$$

Each specie mole fraction was initialized at a chosen time following intake valve closure and a single step global C_nH_m chemistry model was utilized to determine perturbations in the specie mole fractions upon initiation of the injection process. Since the apparent heat release rate does not differentiate between heat transfer and gross burning rate, and typical combustion efficiencies in diesel engines are 99%, a speed up factor was incorporated within the chemistry model to ensure a nearly complete burn and thus a more accurate calculation of the charge specific heat ratio. All experimental pressure traces were conditioned with a digital low pass filter that had a cutoff frequency of typically twice the engine speed preceding heat release analysis and n-hexadecane was chosen as a surrogate fuel for DF-2 based on a recent heat release fuel sensitivity study [18].

FUEL EFFECTS - A commercial DF-2 was employed throughout evaluation of the Ford DIATA engine while a military grade DF-2 was utilized throughout the V903 test schedule. Details of each fuel are given in table 2.

Table 2: Test Fuel Specifications

Fuel Parameter	Engine Configuration	
	Cummins V903	Ford DIATA
Density (kg/m^3)	845	842
Cetane Number	47	53
Net Heating Value (MJ/kg)	42.6	42.8
Hydrogen (% wt.)	12.8	13.25
Sulfur (ppm)	1400	400

PREMIXED PHASE FLAMELET MODEL

The combustion event is idealized as a sequence of three events that has been described in the past as the Large Scale Combustion Model (LSCM) – ignition, consumption of a fuel-air mixing layer, and consumption of mixing controlled fuel-air packets [19]. During the ignition delay, a mixing layer forms on the fuel spray periphery that is comprised of varying local fuel-air ratios and temperature. At some point, a packet or packets of fuel-air charge reach an excited state that results in stabilization of a flame kernel and thus the onset of ignition. Afterward the flame front(s) propagate in rapid fashion throughout the mixing layer consuming packets that reach flammable limits at a rate the order of the fuel injection velocity [20]. This consumption process is commonly referred to as the premixed phase of combustion. After ignition, other fuel packets not originally included within the mixing layer either begin or continue to mix locally with oxidizer. Eventually these packets reach proper proportions and are eventually consumed by the established frame front initiated during

the premixed phase of combustion. The mixing controlled phase of combustion initiates at the onset of consumption of these packets and assumed to occur at stoichiometry.

The LSCM addresses each of these three events and thus includes a premixed phase submodel that is based on the flamelet assumption [1] that was originally employed in homogeneous spark-ignition engines [21-22] and modified for diesel sprays [19] as given below:

$$\frac{dm_{en}}{dt} = FA\rho \ A_f \ (\tilde{u} + S_l + U_{jet})$$

$$\frac{dm_{pb}}{dt} = \frac{m_{en} - m_{pb}}{\tau} \qquad (2)$$

$$\tau = \frac{\delta_t}{S_l} \qquad \frac{\delta_t}{l} \propto Re_l^{-0.5} \qquad Re_l = \frac{\rho \tilde{u} l}{\mu}$$

where m_{en} is the mixing layer charge mass entrainment rate, FA is the average mixing layer fuel-air ratio, ρ is the charge density, A_f is the flame front area, $\tilde{u}$ is the mean turbulence intensity, S_l is the laminar flame speed, U_{jet} is the local jet penetration rate, m_{pb} is the consumed premixed phase fuel mass, τ is the characteristic burning time, δ_t is the Taylor length scale, l is the representative mixing length scale and μ is the charge viscosity. Furthermore, the flame front area and mean turbulence intensity is given below:

$$\tilde{u} = l\omega \qquad A_f = \pi \left[(R' + \delta_{pm})^2 - R'^2\right] \qquad (3)$$

and ω is the bulk mixing rate, R' is the radial distance from the spray centerline to the onset of the shear layer, and δ_{pm} is the premixed fuel-air shear layer thickness ($\delta_{pm} \sim$ spray tip penetration [23]). The representative eddy length scale is chosen as the following inverse relationship:

$$\frac{1}{l} = \frac{1}{B} + \frac{1}{z+d} \qquad (4)$$

where B is the cylinder bore, d is a representative bowl depth, and z is the distance from the piston lip to the fire deck. The bulk mixing rate is determined based on contributions from the injection event, squish flow, swirl, dissipation, and combustion chamber compression-expansion. Fundamentally it is derived from the angular momentum of a representative eddy as shown below:

$$\frac{d\Omega}{dt} = \overset{\bullet}{P}_{inj} + \overset{\bullet}{P}_s + \overset{\bullet}{P}_{sw} - \overset{\bullet}{D}_s \qquad \Omega = \frac{1}{8} m_e \omega l^2$$

$$\frac{dm_e}{dt} = \overset{\bullet}{m}_{inj} + \overset{\bullet}{m}_{sq} \qquad \overset{\bullet}{P}_s = ABS(\overset{\bullet}{m}_{sq} U_{sq} l_{sq})$$

$$\overset{\bullet}{D}_s = a\omega\Omega\exp(-a\omega \ \delta t) \qquad \overset{\bullet}{P}_{inj} = \frac{\overset{\bullet}{m}_{inj} U_{inj} S}{4} \qquad (5)$$

$$\overset{\bullet}{P}_{sw} = \rho \left(\frac{S+L_b}{2}\right)^3 \omega_s^2 \left\{\tan\left(\frac{\theta}{2}\right)\right\}^2 \frac{S^2 - L_b^2}{2}$$

where $\overset{\bullet}{P}_{inj}$ is the injection production term, $\overset{\bullet}{P}_s$ is the squish production term, $\overset{\bullet}{D}_s$ is the dissipation term, m_e is the eddy mass, $\overset{\bullet}{P}_{sw}$ is the swirl production term, $\overset{\bullet}{m}_{inj}$ is the injection rate, $\overset{\bullet}{m}_{sq}$ is the squish mass flow rate, U_{sq} is the average squish velocity, l_{sq} is the squish length scale, a is the dissipation constant, U_{inj} is the injection velocity, δt is the calculation time step, L_b is the break-up length, θ is the spray cone angle, ω_s is the swirl rate, and S is the spray tip penetration distance. The squish mass flow rate is determined based on piston speed, squish area, and bulk density [24] and the squish length is defined as $- (z/2 + I/4)$. Details of each submodel are given by Schihl et al. [19].

Last, the spray formation process is the two zone model of Hiroyasu et al. [25] that is applicable both to the liquid dominated and gaseous regimes. For completeness, this model is given below:

$$t < t_b \qquad S(t) = B \ U_{inj} \ t \qquad t_b = \frac{\alpha \rho_l d_o}{(2c_1 \rho \Delta P)^{0.5}}$$

$$t > t_b \qquad S(t) = 2.95 \left(\frac{\Delta P}{\rho}\right)^{0.25} (d_o t)^{0.5} \qquad (6)$$

where B is a constant, t_b is the break-up time, d_o is the orifice diameter, α and c_1 are break-up constants, ΔP is the orifice pressure drop, and ρ_l is the injected fuel density.

The three major parameters controlling the premixed phase burn rate are the laminar flame speed, spray angle, i.e. flame front area, and the turbulence intensity. The former is a function of the fuel and thermodynamic state of the mixture and fundamentally is described below:

$$S_l = S_{l,o} \left(\frac{T}{T_o}\right)^2 \left(\frac{P}{P_o}\right)^a \left(\frac{O_2}{O_{2,o}}\right)^b \qquad (7)$$

where o-subscripted parameters represent reference conditions, T is the mean cylinder temperature at ignition, P is the cylinder pressure at ignition, O_2 is the oxygen concentration, and a and b are fuel dependent constants. These latter constants are ideally determined through a best fit of experimental data that is currently not available for DF-2 as discussed within the introduction.

Last, the LSCM mixing controlled phase is a characteristic time model that has been extensively discussed in the past [18-19]. Essentially, the mixing time is the conjugation of four time scales – the bulk mixing time, the wall effect, an EGR based oxygen displacement, and an air utilization correction (See references 18 and 19 for more detail.) – that collectively dictate both the mixing and fuel consumption rates. As noted earlier, the consumption rate is controlled by the turbulence intensity.
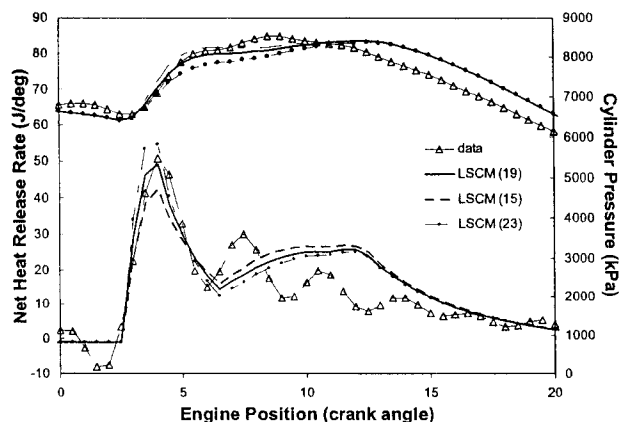
Figure 1: LSCM Laminar Flame Speed Calibration at Light Load for DIATA Engine.

MODEL CALIBRATION PROCEDURE

The philosophy of matching the LSCM generated heat release profiles with each experimental counterpart determined through analysis of in-cylinder pressure data is based on the assumption that mixing is semi-accurately modeled throughout the combustion event. As outlined during the preceding discussion, both the premixed and mixing controlled phases of combustion are intimately related to overall in-cylinder turbulent intensity. Consumption of fuel in the premixed mixing layer is highly dependent on the characteristic burning time that in turn is implicitly dependent on the mean turbulent intensity through modulation of the Taylor scale. The subsequent mixing controlled phase of combustion is explicitly controlled by the mixing rate that is directly linked to the turbulent intensity and the associated mixing length. Thus, successful calibration of the LSCM over a range of operating conditions to determine the laminar flame speed requires matching both the experimental pressure and heat release profiles.

Thus, LSCM was optimized to match experimentally determined profiles through selection of the optimal laminar flame speed over various operating conditions. A priori to this effort, the spray angle was judiciously chosen for each data point based on both past experience and available published data from various sources [26-32]. An example of this process is demonstrated by figure 1 that shows the influence of laminar flame speed on the overall premixed phase behavior. The choice of the larger laminar speed value (23 cm/s) resulted in an over prediction of the peak premixed phase burning rate while choice of the lower laminar flame speed (15 cm/s) has the converse effect. For this particular case, the choice of the optimal laminar flame speed (19 cm/s) matched both the heat release and cylinder pressure profiles in an acceptable manner that implies that LSCM did properly capture the mixing time scales. Additionally, similar analysis is shown for the larger bore engine included in this study as shown in figure 2.
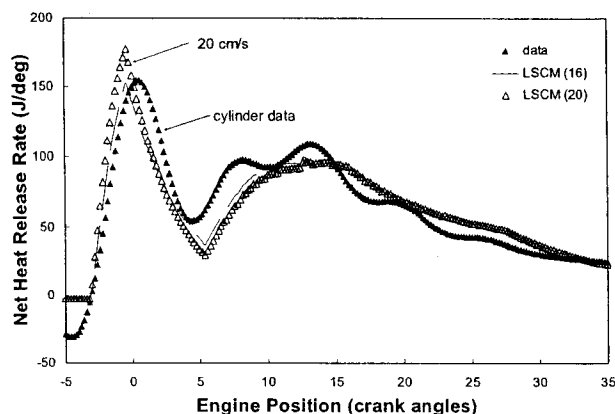

Figure 2: LSCM Laminar Flame Speed Calibration at Half Load for Cummins V903 Engine.

A total of seventy-seven operating points were available for this study but only fifty were accepted and included in this study since twenty-seven of the points did not exhibit a precise enough combination heat release-cylinder pressure LSCM match with the experimental data. A typical acceptable match leads to fairly accurate agreement between experimental and LSCM pressure-heat release profiles and another example of a heat release profile match is shown in figure 3.

RESULTS

The laminar flame speed correlation (equation 7) is a function of charge pressure, temperature, and equivalence ratio. These latter two parameters vary with time during the post-ignition flame spread event since the mixing layer is stratified in both composition and reactant temperature. In order to simplify this complex event, the bulk temperature and pressure, and oxygen concentration at the spray tip at ignition were chosen as representative values throughout the premixed phase of combustion. Furthermore, the spray tip oxygen concentration at ignition was determined based on the
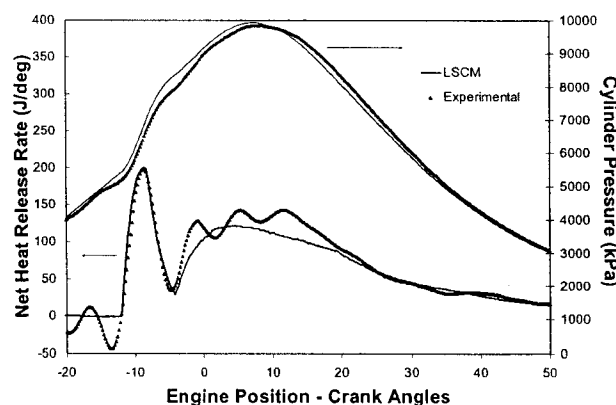

Figure 3: LSCM Laminar Flame Speed Optimization for the Cummins V903 at High Load.
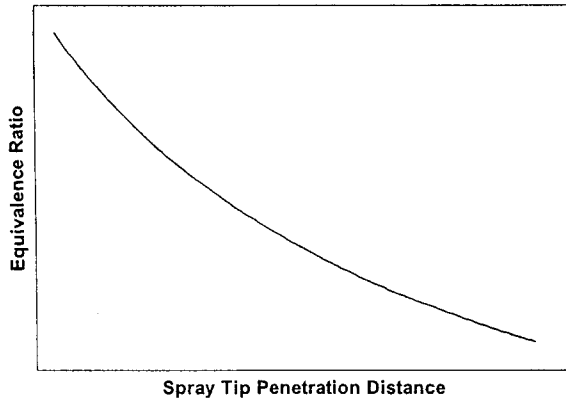
Figure 4: Influence of Spray Tip Penetration Distance on Mean Shear Layer Air-Fuel Ratio.
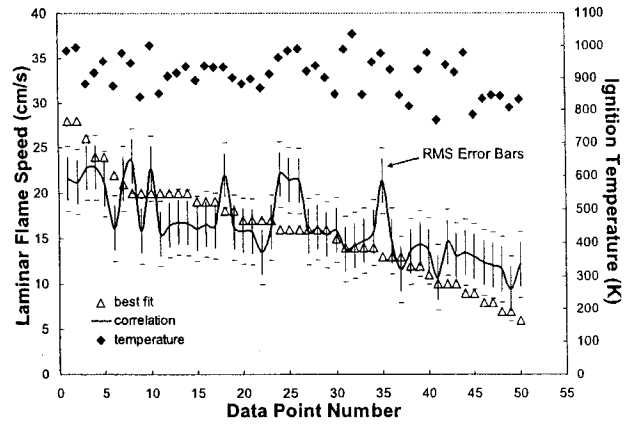

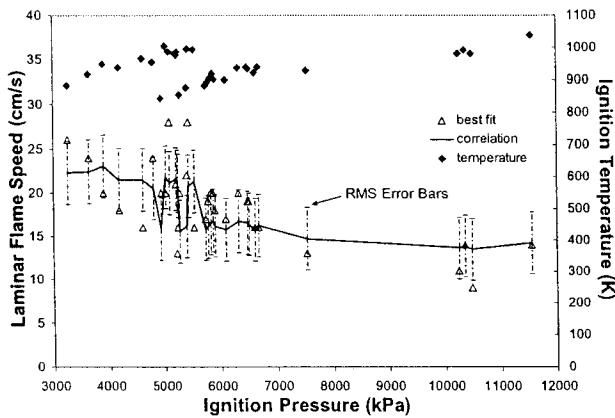Figure 5: Comparison of Laminar Flame Speed Correlation with LSCM Best Fit Values.

Figure 6: Comparison of the Laminar Flame Speed Correlation with the LSCM Best Fit Values for Non-EGR Operating Conditions.

Figure 7: Comparison of the Laminar Flame Speed Correlation with the LSCM Best Fit Values for EGR Operating Conditions.

spray penetration distance at ignition – see figure 4.

The two test fuels employed in this study had similar bulk properties as outlined in table 2 except for the cetane number and sulfur concentration level. Based on this general comparison of fuel properties it was assumed that the reference laminar flame speed at ambient temperature and pressure, and the pressure dependency behavior were identical. Thus, both engine data sets were combined and employed to determine the optimal correlation constants.

The overall behavior of the optimal (best-fit) laminar flame speed and the associated correlation is given in figure 5. Due to the multi-dimensional dependency of the correlation, data is presented in a monotonically decreasing order versus measured cylinder ignition pressure. Inherent in this data set are eighteen EGR points that were acquired from the Ford DIATA experimental study. Note that the best-fit laminar flame speed varies between 6 cm/s and 30 cm/s with an associated bulk ignition temperature ranging from 800 K to 1040 K as dependent on the speed-load operating point. Additionally, the spray tip oxygen mass fraction
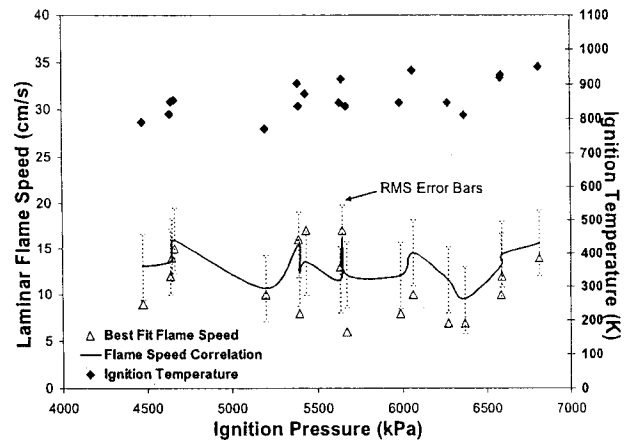
was much less at the lower range of the best-fit flame speed spectrum in part due to EGR that varied between 10% to 45% and the associated lower ignition temperatures versus non-EGR cases. This later observation is apparent by studying the non-EGR and EGR cases as given in figures 6 and 7. Last, cool flame operating conditions were excluded from this study since LSCM does not address low temperature chemistry heat release [19].

The resulting laminar flame speed correlation exhibited a root-mean-square (RMS) error of ±3.6 cm/s in comparison to the best-fit values. Overall only a small portion (six) of the best-fit values fell well outside the RMS error but this shortcoming is not that significant considering a zero-dimensional combustion model (LSCM) was employed in this study. The implication is that LSCM in general captured the bulk mixing profile to sufficiently predict the net heat release profiles in two distinctly different direct-injection diesel engines over a variety of operating conditions. The resulting correlation is given below:

$$S_l = 21 \left(\frac{T}{300} \right)^2 P^{-0.6} \left(\frac{Y_{O_2}}{0.21} \right)^{0.3} \qquad (8)$$

where S_l has units of cm/s, P and T have units of bar and Kelvin, and Y_{O2} is the spray tip oxygen mass fraction.

CONCLUSION

A method to indirectly determine the laminar flame speed was developed for direct injection diesels based on using a zero-dimensional two-phase combustion model to match experimental pressure and heat release data. Data acquired for both light-duty and heavy-duty engines was employed in this study and revealed a laminar flame speed correlation that had realistic trends and magnitude. The correlation is limited to non-cool flame operating conditions since the zero-dimensional combustion model employed in this study did not include low temperature chemistry capability. This correlation maybe employed in three-dimensional flame models used for diesel applications.

ACKNOWLEDGMENTS

REFERENCES

1. Turns, S., **An Introduction to Combustion: Concepts and Applications**, McGraw-Hill Inc., 1996.
2. Kobayashi, H., Tamura, T., Maruta, K., Niioka, T., and Williams, F.A., "Burning Velocity of Turbulent Premixed Flames in a High-Pressure Environment", *Twenty-Sixth Symposium on Combustion*, The Combustion Institute, p. 389, 1996.
3. Andrews, G.E. and Bradley, D., "The Burning Veloctiy of Methane-Air Mixtures", Combustion and Flame, vol. 19, p. 275, 1972.
4. Zhou, M. and Garner, C.P., "Direct Measurements of Burning Velocity of Propane-Air Using Particle Image Velocimetry", *Combustion and Flame*, vol. 106, p. 363, 1996.
5. Daly, C.A., Simmie, J.M., Wurmel, J., Djebaïli, N. and Paillard, C., "Burning Velocites of DiMethyl Ether and Air", *Combustion and Flame*, vol. 125, p. 1329, 2001.
6. Hirasawa, T., Sung, C.J., Yang, Z., Wang, H., and Law, C.K., "Determination of Laminar Flame Speeds of Ethylen/n-Butane/Air Flames Using Digital Particle Image Velocimetry", 2nd Joint Meeting of U.S. Section of the Combustion Institute, Paper No. 138, 2001.
7. Egolfopoulos, F.N., Zhu, D.L., and Law, C.K., "Experimental and Numerical Determination of Laminar Flame Speeds: Mixtures of C2-Hydrocarbons with Oxygen and Nitrogen", *Twenty-third Symposium on Combustion*, The Combustion Institute, p. 513, 1998.
8. Law, C.K., "A Compilation of Experimental Data on Laminar Burning Velocities", **Reduced Kinetic Mechanisms for Applications in Combustion Systems**, edited by N. Peters and B. Rogg, Spring-Verlag, p. 15, 1993.
9. Metghalchi, M. and Keck, J.C., "Burning Velocities of Mixtures of Air with Methanol, Isooctane, and Indolene at High Pressures and Temperatures", Combustion and Flame, vol. 48, p. 191, 1982.
10. Private communication with Southwest Research Institute.
11. Siebers, D., Higgins, B., and Pickett, L., "Flame Lift-Off on Direct-Injection Diesel Fuel Jets: Oxygen Concentration Effects", SAE Paper 2002-01-0890, 2002.
12. Espey, C., Dec, J.E., Litzinger, T.A., and Santavicca, D.A., "Quantitative 2-D Fuel Vapor Concentration Imaging in a Firing D.I. Diesel Engine Using Planar Laser-Induced Rayleigh Scattering", SAE Paper 940682, 1994.
13. Kim, T., Beckman, M.S., Farrell, P.V., and Ghandhi, J.B., "Evaporating Spray Concentration Measurements for Small and Medium Bore Diesel Injectors", SAE Paper 2002-01-0219, 2002.
14. Suzuki, M., Nishida, K., and Hiroyasu, H., "Simultaneous Concentration Measurement of Vapor and Liquid in an Evaporating Diesel Spray", SAE Paper 930863, 1993.
15. Schihl, P., Tasdemir, J., Bryzik, W., and Schwarz, E., 'Simulating the Heat Release Event in Military Diesel Engines", 23rd Army Science Conference, 2002.
16. Schihl, P., Schwarz, E., and Bryzik, W., "Performance Characteristics of a Low Heat Rejection Direct-Injection Military Diesel Engine Retrofitted With Thermal Barrier Coated Pistons", Trans. Of ASME, *Journal of Engineering for Gas Turbines and Power*, vol. 123, p. 644, 2001.
17. Kanimoto, T., Minagawa, T., and Kobori, S., "A Two-Zone Model Analysis of Heat Release Rate in Diesel Engines", SAE Paper 972959, 1997.
18. Schihl, P., Tasdemir, J., Schwarz, E., and Bryzik, W., "Development of a Zero-Dimensional Heat Release Model for Application to Small Bore Diesel Engines", SAE Paper 2002-01-0073, 2002.
19. Schihl, P.J., Atreya, A., and Bryzik, W., "Simulation of Combustion in Direct-Injection Low Swirl Heavy-Duty Type Diesel Engines", SAE Paper 1999-01-0228, 1999.
20. Balles, E.N. and Heywood, J.B., "Spray and Flame Structure in Diesel Combustion", Trans. Of ASME,

Journal of Engineering for Gas Turbines and Power, vol. 111, p. 451, 1989.

21. Blizzard, N.C. and Keck, J.C., "Experimental and Theoretical Investigation of Turbulent Burning Model for Internal Combustion Engines", SAE Paper 740191, 1974.

22. Tabaczynski, R., Ferguson, C., and Radhakishnan, K., "A Turbulent Entrainment Model for Spark-Ignition Engine Combustion", SAE Paper 770647, 1977.

23. Dimotakis, P.E., "Turbulent Free Shear Layer Mixing and Combustion", **High Speed Flight Propulsion Systems**, edited by S.N.B. Murthy and E.T. Curran, *Progress in Astronautics and Aeronautics*, vol. 137, 1991.

24. Heywood, J.B., **Internal Combustion Engine Fundamentals**, McGraw-Hill, Inc., 1988.

25. Hiroyasu, H. and Arai, M., "Fuel Spray Penetration and Spay Angle in Diesel Engines", Trans. of the SAE of Japan, 21, p. 5-11, 1980.

26. Su, T.F., Farrell, P.V., and Nagarajan, R.T., "Nozzle Effect on High Pressure Diesel Injection", SAE Paper 950083, 1995.

27. Hiroyasu, H and Arai. M., "Structures of Fuel Sprays in Diesel Engines", SAE Paper 900475, 1990.

28. Ruiz, F. and Chigier, N., "Parametric Experiments on Liquid Jet Atomization Spray Angle", Atomization and Sprays, vol. 1, p. 23, 1991.

29. Montgomery, D.T., Chan, M., Chang, C.T., Farrell, P.V., and Reitz, R.D., "Effect of Injector Nozzle Hole Size and Number of Spray Characteristics and the Performance of a Heavy Duty D.I. Diesel Engine", SAE Paper 962002, 1996.

30. von Kuensberg Sarre, C., Kong, S.-C., and Reitz, R.D., "Modeling the Effects of Injector Nozzle Geometry on Diesel Sprays", SAE Paper 1999-01-0912, 1999.

31. Han, J.-S., Wang, T.C., Xie, X.B., Lai, M.-C., Henein, N.A., Harrington, D.L., Pinson, J., and Miles, P., "Dynamics of Multiple-Injection Fuel Sprays in a Small-bore HSDI Diesel Engine", SAE Paper 2000-01-1256, 2000.

32. Bae, C. and Kang, J., "Diesel Spray Development of VCO Nozzles for High Pressure Direct-Injection", SAE Paper 2000-01-1254.

DEFINITIONS, ACRONYMS, ABBREVIATIONS

DF-2: diesel fuel number 2

RMS: root-mean-square